A Novel Layered QG model

Neil Burrell

1 Introduction

The earth's ocean is a complicated fluid system. It is affected by the rotation of the earth, the density stratification due to temperature and salinity, and many other factors. These processes combine to act on an extremely wide range of length-scales, from centimeters to thousands of kilometers. One notable simplification is that the ocean is tremendously more shallow than it is wide. But the assumption that the ocean is two-dimensional is overly restrictive and does not capture important dynamical processes.

We concern ourselves here with the observation of a correlation in the energy-containing scales of the ocean with the first Rossby deformation radius. This correlation appears in observations of the sea surface using the TOPEX/POSEIDON satellite [1, 2] and also in models [3]. The processes which cause eddy energies in the ocean come to equilibrate at this horizontal scale are not well understood. It is the fully nonlinear development of ocean eddies (presumably created through wind stress forcing at the surface) that determines this scale. In addition, the effect of vertically non-uniform stratification on the downward propagation (barotropization) of energy are not clear. Typical models of ocean turbulence assume vertically homogeneous stratification, with correspondingly more uniform dynamics throughout the layer.

Smith and Vallis [4, 5] investigate these questions in the context of a non-uniformly stratified, three-dimensional ocean using quasigeostrophic (QG) dynamics. The surface-intensified stratification that they use leads to surface-localized potential vorticities. In an effort to create a simpler model for these processes, we consider a two-layer QG system in which the lower layer has no potential vorticity. In section 2 we review layered QG models in general. Then in sections 3 and 4 we examine the simplified two-layer model and its consequences for eddy evolution using numerical simulations. We present our conclusions in section 5.

2 Layered Quasigeostrophic Models

Consider a nearly incompressible, rotating, stratified fluid. All of the models that we consider here will neglect the meridional variation in the Coriolis parameter that is present

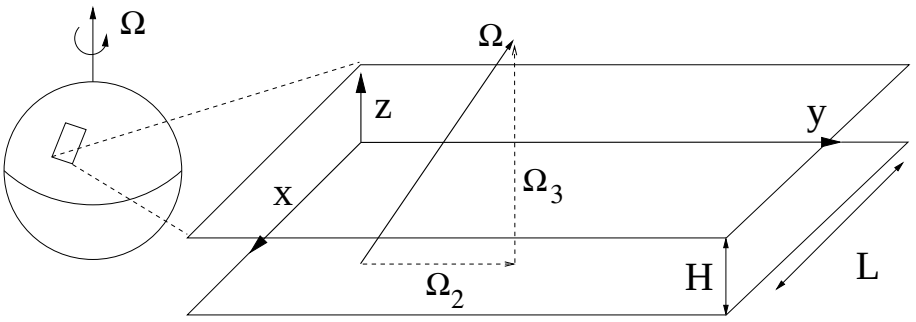

Figure 1: The f-plane geometry.

on a rotating sphere (see figure 1). On this f-plane, the Boussinesq equations are

$$D_t \boldsymbol{u} + 2\Omega(\hat{\Omega} \times \boldsymbol{u}) = -\frac{\nabla p}{\rho_0} + b\hat{\boldsymbol{z}} + \frac{\mu}{\rho_0}\Delta \boldsymbol{u} \tag{1a}$$

$$D_t b + N^2(z) w = \kappa \Delta b \tag{1b}$$

$$\nabla \cdot \boldsymbol{u} = 0 \tag{1c}$$

where the dependent variables are the fluid velocity $\boldsymbol{u}$, the pressure p and the buoyancy anomaly $b = -g\rho/\rho_0$. The parameters are the rotation rate 2Ω, the typical background density ρ_0, the buoyancy frequency $N^2 = -(g/\rho_0)(\mathrm{d}\rho/\mathrm{d}z)$ for a background density $\bar{\rho}$ and the momentum and mass diffusivities, ν and κ respectively. Non-dimensionalizing these equations by $\boldsymbol{u} \sim U$, $\boldsymbol{x} \sim L$, , $b \sim B$, $p \sim P$ and $N^2(z) = N_0^2 S(z)$ we have

$$D_t \boldsymbol{u} + \frac{1}{\mathrm{Ro}}\hat{\Omega} \times \boldsymbol{u} = -\bar{P}\nabla p + \Gamma b\hat{\boldsymbol{z}} + \frac{1}{\mathrm{Re}}\Delta \boldsymbol{u}, \tag{2a}$$

$$D_t b + \frac{S(z)}{\Gamma \mathrm{Fr}^2} w = \frac{1}{\mathrm{Pe}}\Delta b, \tag{2b}$$

$$\nabla \cdot \boldsymbol{u} = 0, \tag{2c}$$

where the Reynolds number $\mathrm{Re} = (UL)/\nu$ measures the strength of inertia relative to viscosity, the Peclet number $\mathrm{Pe} = (UL)/\kappa$ compares inertia to buoyancy diffusion, the Froude number $\mathrm{Fr} = U/(N_0 L)$ measures buoyancy relative to inertia and the Rossby number $\mathrm{Ro} = U/(2\Omega L)$ compares the rotational timescale to the dynamical timescale. There are two additional non-dimensional parameters $\bar{P} = P/(U^2\rho_0)$ and $\Gamma = (BL)/U^2$ that measure the strength of their respective terms of the equations.

Since the ocean is vastly shallower than it is wide, even at the horizontal scales considered here, we consider an asymptotic expansion in the aspect ratio $\epsilon = H/L$. In the ocean, the Rossby number is also small so we set $\mathrm{Ro} = \epsilon$. We neglect the effects of diffusion, by setting $\mathrm{Re} = \mathrm{Pe} = \infty$. Froude numbers in the ocean are smaller than the Rossby numbers, so we choose $\mathrm{Fr} = \epsilon^2$ and for the other two parameters we take $\Gamma = \epsilon^{-2}$ and $\bar{P} = \epsilon^{-1}$ to give the hydrostatic and geostrophic balances at leading order. Expanding the dependent variables in asymptotic series ($\boldsymbol{u} = \boldsymbol{u}_0 + \epsilon\boldsymbol{u}_1 + \epsilon\boldsymbol{u}_2 + \ldots$, etc.) and collecting terms of the same order

we have the following balances from the momentum equations,

$$O(\epsilon^{-2}): \quad -\partial_z p_0 + b_0 = 0 \tag{3a}$$
$$O(\epsilon^{-1}): \quad \hat{\Omega} \times \boldsymbol{u}_0 = -\nabla_\perp p_0 + \hat{\boldsymbol{z}}(b_1 - \partial_z p_1) \tag{3b}$$
$$O(1): \quad D_t^0 \boldsymbol{u}_0 + \hat{\Omega} \times \boldsymbol{u}_1 = -\nabla_\perp p_1 + \hat{\boldsymbol{z}}(b_2 - \partial_z p_2) \tag{3c}$$

the buoyancy equation,

$$O(\epsilon^{-2}): \quad S(z) w_0 = 0 \tag{3d}$$
$$O(\epsilon^{-1}): \quad w_0 \partial_z b_0 + S(z) w_1 = 0 \tag{3e}$$
$$O(1): \quad D_t^0 b_0 + w_1 \partial_z b_0 + S(z) w_2 = 0 \tag{3f}$$
$$\tag{3g}$$

and the continuity equation

$$O(1): \quad \nabla_\perp \cdot \boldsymbol{u}_0 = 0 \tag{3h}$$
$$O(\epsilon): \quad \nabla_\perp \cdot \boldsymbol{u}_1 + \partial_z w_2 = 0. \tag{3i}$$

From (3d) and (3e) we see that the fluid velocities are all horizontal. The hydrostatic balance is present at leading order in (3a) and the geostrophic balance in the x- and y-components of (3b). The incompressibility condition (3h) leads us to a streamfunction $\boldsymbol{u}_0 = \hat{\boldsymbol{z}} \times \nabla \psi_0$. The geostrophic and hydrostatic balances relate that streamfunction to the pressure and buoyancy fields at leading order: $p_0 = \Omega_3 \psi_0$ and $b_0 = \Omega_3 \partial_z \psi_0$. Taking the curl of (3c) and using (3i) to relate w_2 and $\boldsymbol{u}_1$ we have two closed equations for ψ and w_2

$$D_t^0 \nabla_\perp^2 \psi_0 - \Omega_3 \partial_z w_2 = 0 \tag{4a}$$
$$D_t^0 \Omega_3 \partial_z \psi_0 + S(z) w_2 = 0. \tag{4b}$$

Finally, eliminating w_2 and dropping the 0 subscripts we have the quasigeostrophic (QG) equations

$$D_t q = \partial_t q + J(\psi, q) = F \tag{5a}$$
$$q = \nabla^2 \psi + \Omega_3 \partial_z \left(\frac{1}{S(z)} \Omega_3 \partial_z \psi \right), \tag{5b}$$

where F represents any forcing or dissipation in the system.

We will use these equations as the starting point of our investigations. It is important to note that even in the three-dimensional case there is no vertical velocity; all fluid motion is in horizontal planes. If there is no dissipation, $F = 0$, then the QG equations express the conservation of the *potential vorticity* q on fluid elements. Additionally, there are two global conserved quantities: the *energy*

$$\mathcal{E} = -\frac{1}{2} \int_{\mathbb{R}^3} q\psi \, \mathrm{d}\boldsymbol{x} \tag{6}$$

and the *enstrophy*

$$\mathcal{Z} = \int_{\mathbb{R}^3} q^2 \, \mathrm{d}\boldsymbol{x}. \tag{7}$$

Related to the energy and enstrophy are the energy and enstrophy *spectra* defined by $\mathcal{E} = \int E(\kappa)\,\mathrm{d}\boldsymbol{k}$ and $\mathcal{Z} = \int Z(\kappa)\,\mathrm{d}\boldsymbol{k}$. We can define a mean wave number by the centroid of the energy spectrum

$$\kappa_m = \frac{1}{\mathcal{E}} \int \kappa E(\kappa)\,\mathrm{d}\boldsymbol{k}. \tag{8}$$

In the absence of vertical variation, these are just the equations for two-dimensional fluid dynamics where q is the ordinary vorticity and ψ is the streamfunction of the flow. The dynamics of this type of flow are well known (see, for example [6, 7, 8, 9, 10, 11]). For the case of small F, energy is approximately conserved and moves to larger scales in an inverse cascade, enstrophy is not conserved and participates in a direct cascade to smaller scales and for unforced flow the evolution is dominated by the interaction of coherent vortices (which may be studied independently [12, 13, 14]). A quantitative scaling theory for the regime dominated by coherent vortices predicts algebraic evolution for many of the flow characteristics, including enstrophy, vortex number, vortex size and vortex amplitude [15, 9]. We will use these self-similarity properties later for our novel model.

The smallest amount of additional vertical variation that we can admit is a two-layer quasigeostrophic model. Considering two layers of fluid with different densities (see figure 2) the QG equations reduce to

$$\partial_t q_i + J(\psi_i, q_i) = 0, \tag{9a}$$

$$q_1 = \nabla^2 \psi_1 + F_1(\psi_2 - \psi_1), \tag{9b}$$

$$q_2 = \nabla^2 \psi_2 + F_2(\psi_1 - \psi_2) \tag{9c}$$

$$F_i = \frac{f^2}{g' H_i}, \quad f = 2\Omega_3, \quad g' = g\frac{\rho_2 - \rho_1}{\rho_2}.$$

(See [16] or [17] for a derivation of these equations.) In the interest of further simplicity, assume $H_2 \to \infty \Leftrightarrow F_2 = 0$. Then the motion in the lower layer is decoupled from that in the upper layer (although not vice-versa). If we assume that this infinitely deep lower layer was initially at rest, then it will always be at rest with $\psi_2 = 0$. This quiescent lower layer then has no effect on the upper layer and we get the *one-and-a-half layer* QG equations (also called the *equivalent barotropic* QG equations)

$$D_t q_1 = 0 \tag{10a}$$

$$q_1 = (\nabla^2 - F_1)\psi_1. \tag{10b}$$

The parameter F_1 is related to an intrinsic length scale of this flow, the *Rossby deformation radius*, $k_1^{-1} = F_1^{-1/2}$. The dynamics of this system in the case of unforced, decaying turbulence are similar to that of the one-layer equations for short times with the formation and interaction of coherent vortices. As the vortices grow to the size of the deformation radius, their motion begins to slow down [18, 19, 20]. This stops the inverse cascade of energy at that scale, in contrast to the one layer case where the inverse cascade continues to the largest scales in the problem.

Neither the one layer QG model nor the equivalent barotropic model can adequately explain the energetic distribution in the world's oceans. The inverse cascade in 2D turbulence moves to the largest available scales. In fact, there is no intrinsic length scale in

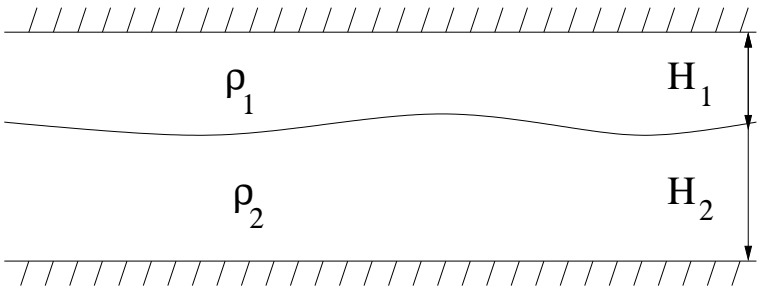

Figure 2: Two fluid layers.

the system. The one-and-a-half layer model does have a distinguished length scale, the deformation radius, but the energy cascade stops completely at that scale. The one layer model is overly simplistic, containing no contributions from rotation or stratification, nor any variation with depth. The addition of an infinitely deep lower layer contributes some of the dynamical features of the ocean, namely the rotational and stratification effects of the deformation radius, but at the cost of the long-time evolution of the flow. This limitation arises from the blatantly unrealistic assumption of infinite depth in the lower layer. For these reasons, we seek a slightly more complicated model that will retain essential features of the oceanic evolution, in particular the distinguished role of the first Rossby deformation radius.

3 The Finite-depth One-and-a-half Layer Model

In our derivation of the equivalent barotropic model, we assumed that the lower layer was infinitely deep. If we relax that assumption, then we cannot continue to insist that $\psi_2 = 0$ for all time. For any finite depth, any motion in the upper layer will induce a flow in the initially quiescent lower layer. Fundamentally, this is because the fluid velocity in the lower layer is not a materially conserved quantity: it may evolve with time. On the other hand, the potential vorticity in the lower layer q_2 is conserved, so if the flow initially has $q_2 = 0$ then it will for all time, irregardless of the motion of the upper or lower layers. This assumption is also consistent with observations [21] which show no potential vorticity signal below eddies in the North Atlantic. Finally, in the three dimensional calculations of Smith and Vallis [4, 5] they compute the eigenfunctions ϕ_i for the vertical structure of the 3D QG equations,

$$\partial_z \left(\frac{1}{S(z)} \partial_z \right) \phi_i = -\lambda_i^2 \phi_i, \tag{11}$$

for a surface-intensified stratification profile and they are quite small at large depths. One limitation of the assumption that $q_2 = 0$ for all time is that it there cannot be any bottom friction present in our model, because that would break the conservation of potential vorticity in the lower layer.

Proceeding with the assumption that $q_2 = 0$, (9c) just expresses a relation between the two streamfunctions

$$\nabla^2 \psi_2 + F_2(\psi_1 - \psi_2) = 0. \tag{12}$$

Thus, given ψ_1 we can solve this equation for ψ_2 in terms of $\hat{\psi}_1$ the Fourier transform of ψ_1

$$\psi_2(\boldsymbol{x},t) = \int \frac{F_2}{F_2+\kappa^2}\hat{\psi}_1 e^{-i\boldsymbol{k}\cdot\boldsymbol{x}}\,\mathrm{d}\boldsymbol{k} \tag{13}$$

where $\boldsymbol{k}$ is the horizontal wavenumber and $\kappa = |\boldsymbol{k}|$. We will represent this solution schematically by

$$\psi_2 = \frac{F_2}{F_2-\nabla^2}\psi_1 \tag{14}$$

where (13) is meant by this symbol in all cases. Having solved for ψ_2 (9b) and (9a) are now a closed set of equations for the motion of the upper layer

$$D_t q_1 = 0, \tag{15a}$$

$$q_1 = \left(\nabla^2 - F_1 + \frac{F_1 F_2}{F_2-\nabla^2}\right)\psi_1. \tag{15b}$$

We refer to these as the *finite-depth one-and-a-half layer* QG equations. Note that in contrast to the model with an infinitely-deep lower layer, the lower layer is not at rest in this model, but instead moves with exactly the relative vorticity $\nabla^2\psi_2$ necessary to cancel the vorticity added to the layer by stretching of the background planetary vorticity, $F_2(\psi_1-\psi_2)$. These equations also contain both of the models talked about previously: if $F_1 = 0$ then we recover the one layer model and if $F_2 = 0$ we have the same equations as the one-and-a-half layer model. As far as we know, this model has not been studied for its turbulent cascade properties as we do here. Since it is a special case of the two-layer QG equations, solutions of this type have certainly appeared, most notably in studies of the merging of baroclinic vortices [22, 18, 23, 24].

4 Spin-down Simulations

The main component of this study is a series of numerical simulations of layered QG equations with a single active layer. The numerical code is pseudospectral in space and leapfrog in time. An isotropic truncation is applied with wavenumbers with $\kappa \le \kappa_{\max} = 176$. When computing the nonlinear term, dealiasing is used, keeping wavenumbers up to $(3/2)\kappa_{\max}$. Dissipation is present in the form of hyperdiffusion $F = -\nu\nabla^8 q$ (as in [4]). All of the simulations presented here use $\nu = 1.43\times10^{-17}$ which was chosen to absorb the direct cascade of enstrophy while dissipating as little energy as possible. The initial vorticity field is a random-phase realization with an initially narrow-band energy spectrum $E(\kappa) \propto \kappa^6/(\kappa+2\kappa_0)^{18}$ with $\kappa_0 = 30$ and the normalization that $\mathcal{E}(t=0) = 0.5$. The simulations continue up to $t = 80$.

Figure 3 shows representative evolutions of energy, enstrophy and κ_m for the one layer model. Over the length of the simulation, the energy falls to approximately 86% of its initial value while the enstrophy declines by a factor of over 60. The decrease in κ_m is evidence of the inverse cascade of energy to larger scales (lower wavenumbers). Figure 4 shows the vorticity field for the one layer model. As time progresses, there are fewer, larger coherent vortices. The same quantities are shown in figures 5 and 6 for the equivalent barotropic model with $k_1 = 15$. Here by comparison, the coherent vortices fill much more of the domain

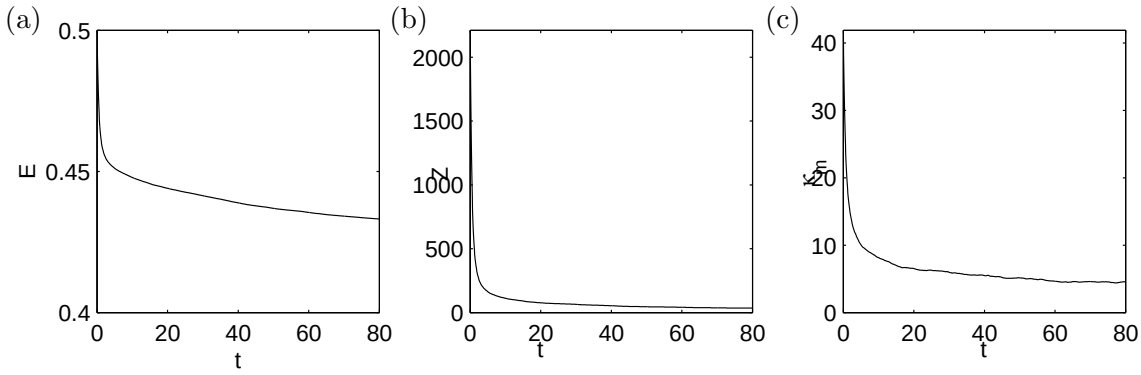

Figure 3: Time series of (a) $\mathcal{E}$, (b) $\mathcal{Z}$ and (c) κ_m for the one layer equations.

than in figure 4. The stopping of the inverse cascade of energy at a scale near the Rossby radius of deformation can be seen in the evolution of κ_m in figure 5.

For the finite-depth model, corresponding data are shown in figures 7 and 8 for $k_1 = 24$ and $k_2 = 12$. A number of notable features are present in these latter simulations. The inverse cascade of energy continues for the finite-depth case where it did not for the equivalent barotropic model ($\kappa_m(t = 80) = 7.5$ and $\kappa_m(t = 80) = 10.1$ respectively). Also, the coherent vortices for the finite-depth model fill more of the space than in the one layer model (figure 4) but less space than in the equivalent barotropic model (figure 6). For increasing values of $\lambda = 1 + F_1/F_2$ the vortices fill more of the domain and are less circular (see figure 9). This is consistent with the position of the finite-depth model as intermediate between the other two models (in the sense that the one layer model corresponds to $\lambda = 1$ and the equivalent barotropic model to $\lambda = \infty$). Finally, for the time evolution of this model: vortex dipoles are more active than in either of the other two models and vortex motions are slower than in the one-layer model but faster than in the equivalent barotropic model.

4.1 Vigorous Vortex Dipoles

To analyze the apparent vigor of close associations of two opposite signed vortices, we consider the induced velocity field for a point charge of potential vorticity. This profile is closely related to those of hetons [25]. Hogg and Stommel give the following solution in the special case $F_1 = F_2$. The azimuthal velocity field is

$$v_\theta(r) = \frac{1}{\lambda}\left(\frac{1}{r} + \frac{F_1}{F_2} k_R K_1\left(k_R r\right)\right) \tag{16}$$

where $k_R = (F_1 + F_2)^{-1/2}$, $\lambda = 1 + F_1/F_2$ and $K_1(z)$ is the modified Bessel function of the second kind. While the vortices in our simulations are not point vortices, this solution should still hold outside of the cortex core, as in the case of the Rankine vortex for the one-layer model. For $r \ll 1/k_R$ the limiting behavior of this velocity is $v_\theta \sim (1/r)$ while for $r \gg 1/k_R$, $v_\theta \sim (1/\lambda)(1/r)$. Since $\lambda \geq 1$ the far-field velocity of a point vortex in

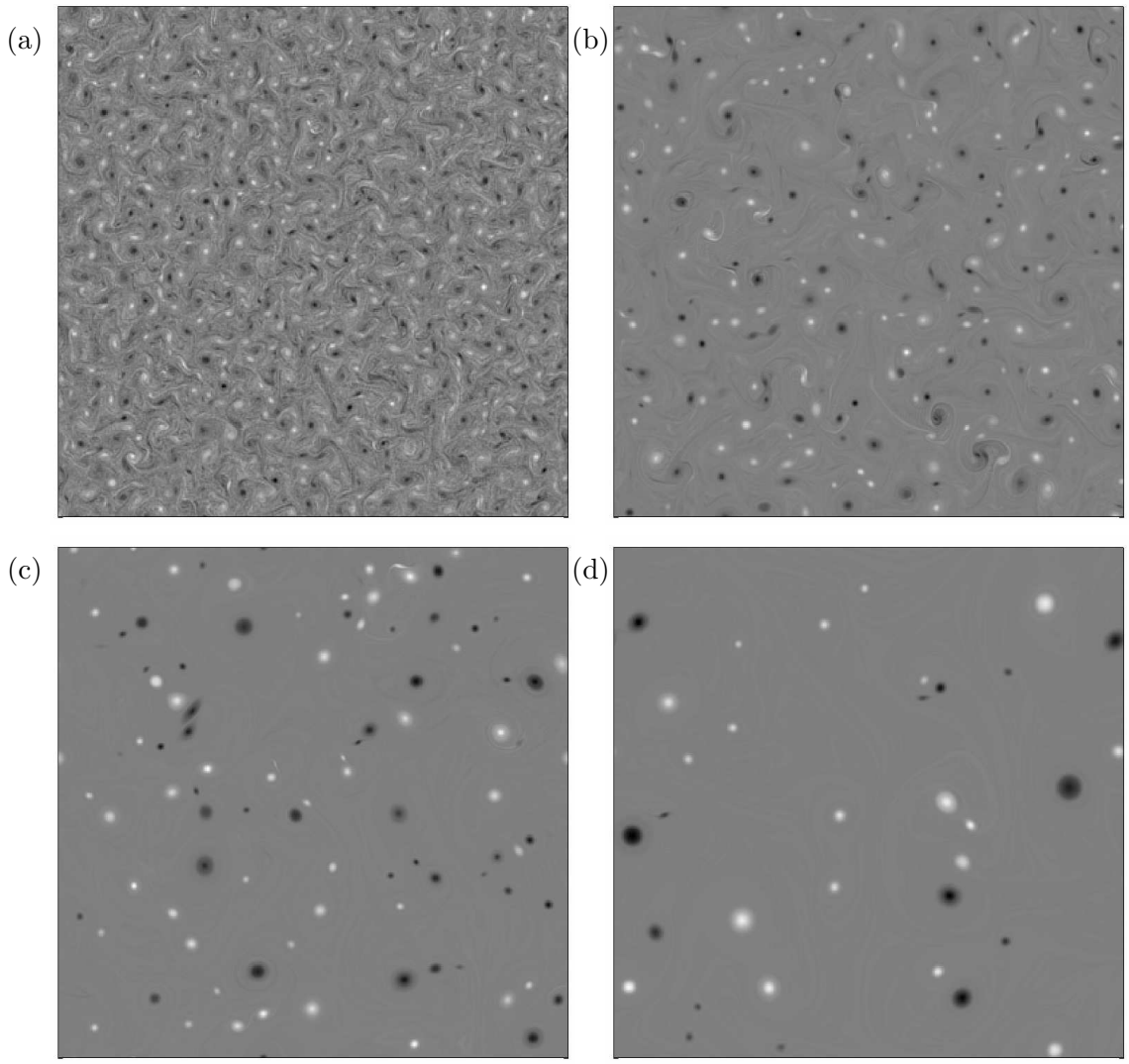

Figure 4: Vorticity field $q_1(x, y)$ at (a) $t = 1$, (b) $t = 5$, (c) $t = 20$ and (d) $t = 80$ for the one layer equations. Lighter colors represent higher vorticities.

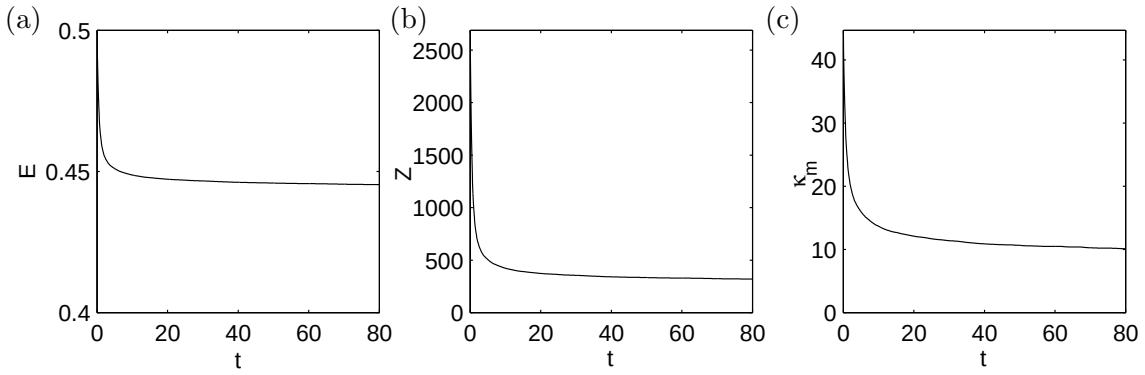

Figure 5: As in figure 3, but for the equivalent barotropic model with $k_1 = 15$.

the finite-depth one-and-a-half layer model is smaller than the near-field velocity. This explains the heightened activity of vortex dipoles in the simulations of these equations. When two opposite signed vortices come close together under the influence of the other vortices in the system, their mutual interaction is strengthened by a factor of λ, resulting in a (possibly dramatic) increase in their activity for the time of their close approach. The increased activity of vortex dipoles also leads to an increased number of dipole/dipole exchange interactions, where two dipoles collide and rebound having exchanged partners.

4.2 Vortex slowdown and self-similarity

A complementary view to the fundamentally physical space approach in section 4.1 is provided by examining the properties of the equations in Fourier space. We will see that there is an intimate connection between these two approaches in the form of the potential vorticity inversion operator. Acting between the Fourier transforms $\hat{q}_1(\boldsymbol{k})$ and $\hat{\psi}_1(\boldsymbol{k})$ this operator takes the form

$$\hat{q}_1 = \left(-\kappa^2 - F_1 + \frac{F_1 F_2}{F_2 + \kappa^2} \right) \hat{\psi}_1. \tag{17}$$

For short scales, when $\kappa \gg F_1^{1/2}$, $\hat{q}_1 \approx -\kappa^2 \hat{\psi}_1$ which is the same form of the operator as we would see in the one layer model where $q = \nabla^2 \psi$. At much larger scales, where $\kappa \ll F_2^{1/2}$, $\hat{q}_1 \approx -\kappa^2 \lambda \hat{\psi}_1$. The appearance of λ in the operator for the large scale interactions in spectral space is parallel to that of the factor of $1/\lambda$ in the velocity profile of a point vortex at large distances. To see this effect, note that if we rescale $q = l\psi \rightarrow q' = \gamma q = \gamma L \psi$, then the original equation for the material conservation of potential vorticity

$$\partial_t q + J(\psi, q) = 0$$

is invariant if we rescale time by $t' = t/\gamma$

$$\partial_{t'} q' + J(\psi, q') = 0.$$

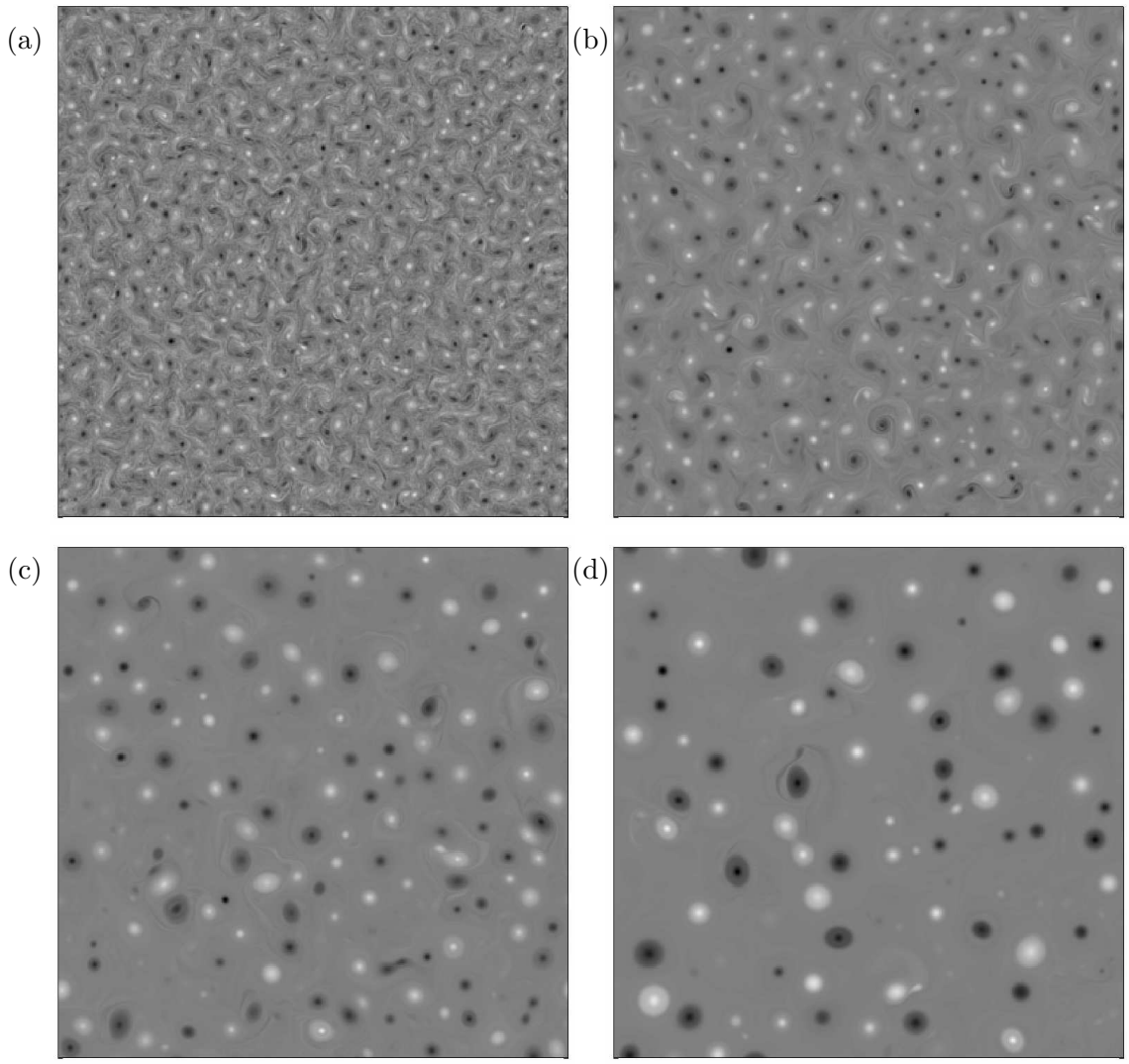

Figure 6: As in figure 4, but for the equivalent barotropic model with $k_1 = 15$.

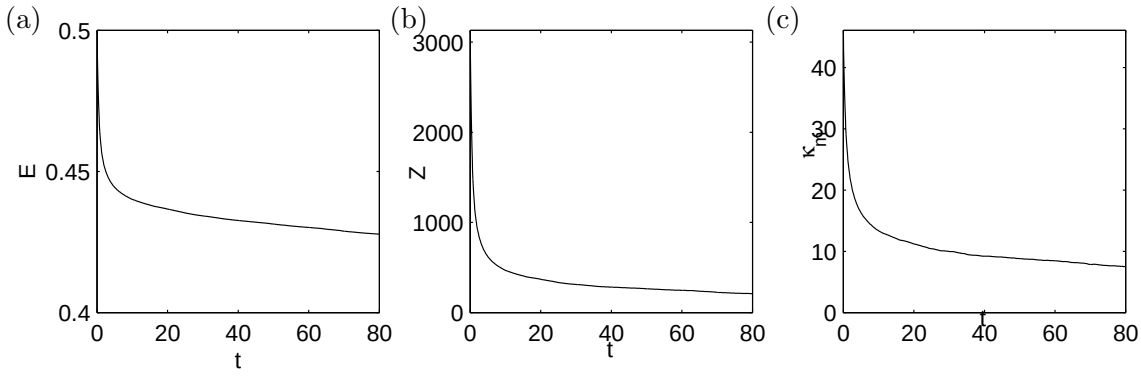

Figure 7: As in figure 3, but for the finite-depth model with $k_1 = 24$, $k_2 = 12$.

From this we can see that any factor that intrudes in the relationship between ψ and q acts analogously to slowing down time by that same factor. Time also slows down by that factor when we consider the reduction of velocity v_θ at large distances from a point vortex.

We can go further with the idea of rescaling time in our evolution equation by re-writing

$$\begin{aligned}\hat{q}_1 &= -\kappa^2 \left(1 + \frac{F_1}{\kappa^2} - \frac{F_1 F_2}{\kappa^2 \left(F_2 + \kappa^2\right)}\right) \hat{\psi}_1 \\ &= -\kappa^2 \gamma(\kappa) \hat{\psi}_1, \end{aligned} \tag{18}$$

where $\gamma(\kappa)$ is the factor by which the finite-depth PV inversion operator differs from that of the operator for the one layer model. This function γ then determines a *scale-dependent* factor by which the evolution of the system should slow down. Note that $\lim_{\kappa\to\infty} \gamma(\kappa) = 1$, $\gamma(0) = \lambda$, consistent with what we saw earlier for small and large scales. This slowing down of time should be apparent in our modified system in the self-similar evolution of the flow. In this regime, $\kappa_m \sim (t/\bar{\gamma})^\alpha$ for some factor $\bar{\gamma}$. While it is not certain that such a self-similar regime exists, the apparent power-law behavior of κ_m for a range of values of λ (figure 10) suggest that it does. From a fit to this data we can determine a value for $\bar{\gamma}$ as a function of λ as shown in figure 11. If all of the energy of the flow were at the largest scales then we would expect $\bar{\gamma} = \lambda$ in accordance with the limit of $\gamma(\kappa)$ for small κ. Clearly this is not a good prediction for $\bar{\gamma}$, except for cases of small λ where most of the energy is at larger scales. A better prediction is given by considering the value of γ for the wavenumber that contains the most energy, as measured by κ_m at the end of the simulation. (κ_m changes by very little over the final half of the simulation.) In fact, the good agreement between these two measures of the slowing down of time is support for the interpretation of $\gamma(\kappa)$ that we gave earlier.

4.3 Reduced axisymmetrization

Another feature of the finite-depth one-and-a-half layer model that is seen in the simulations is a declining tendency for coherent vortices to become axisymmetric with increasing values of λ (figure 9). The process of axisymmetrization is important because it is thought to

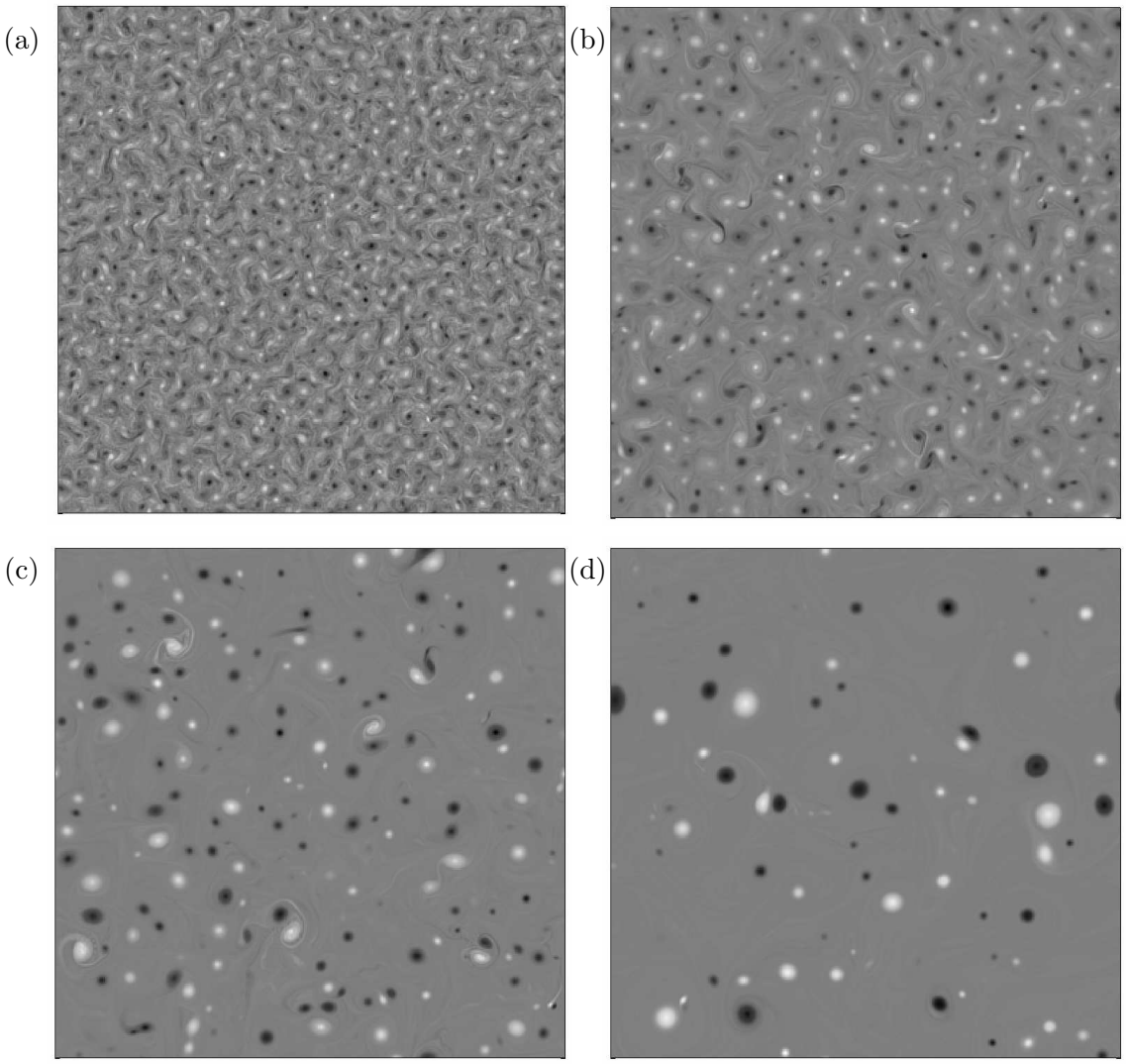

Figure 8: As in figure 4, but for the finite-depth model with $k_1 = 24$, $k_2 = 12$.

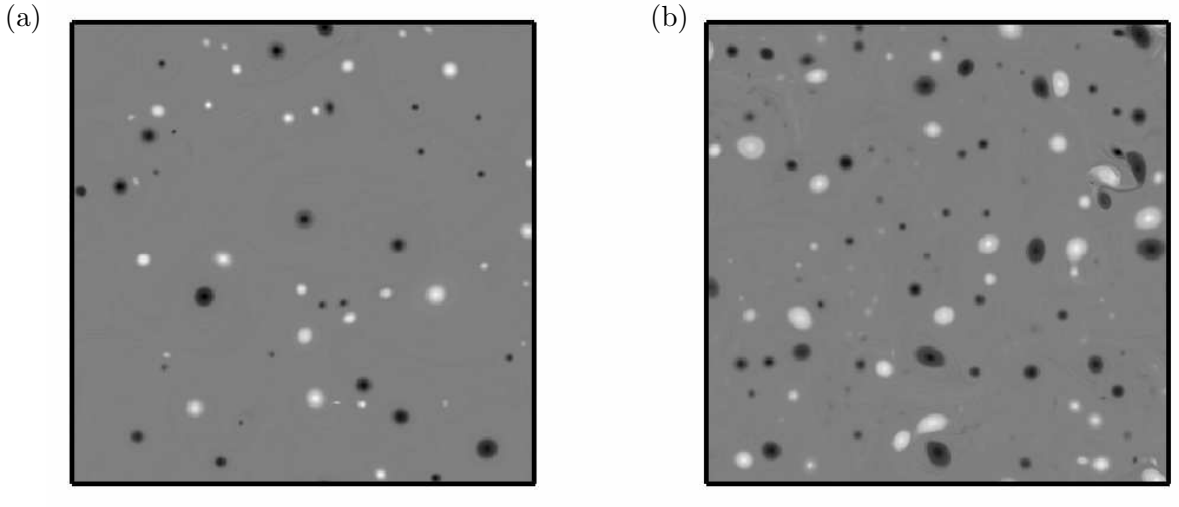

Figure 9: The final vorticity field for (a) $\lambda = 2$ and (b) $\lambda = 17$.

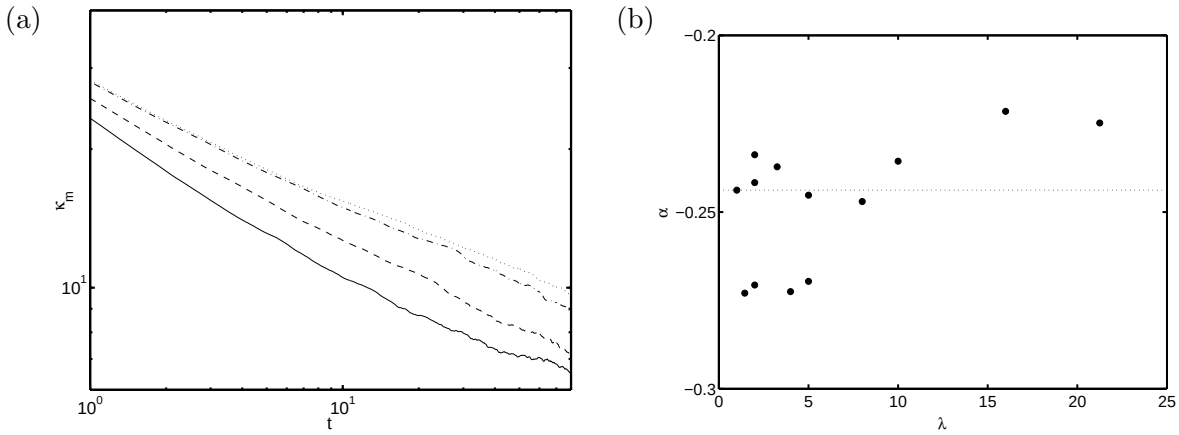

Figure 10: (a) κ_m vs time for $\lambda = 2$ (solid line), $\lambda = 4$ (dashed line), $\lambda = 9$ (dash-dotted line) and $\lambda = 17$ (dotted line). (b) Decay exponent α as a function of λ.

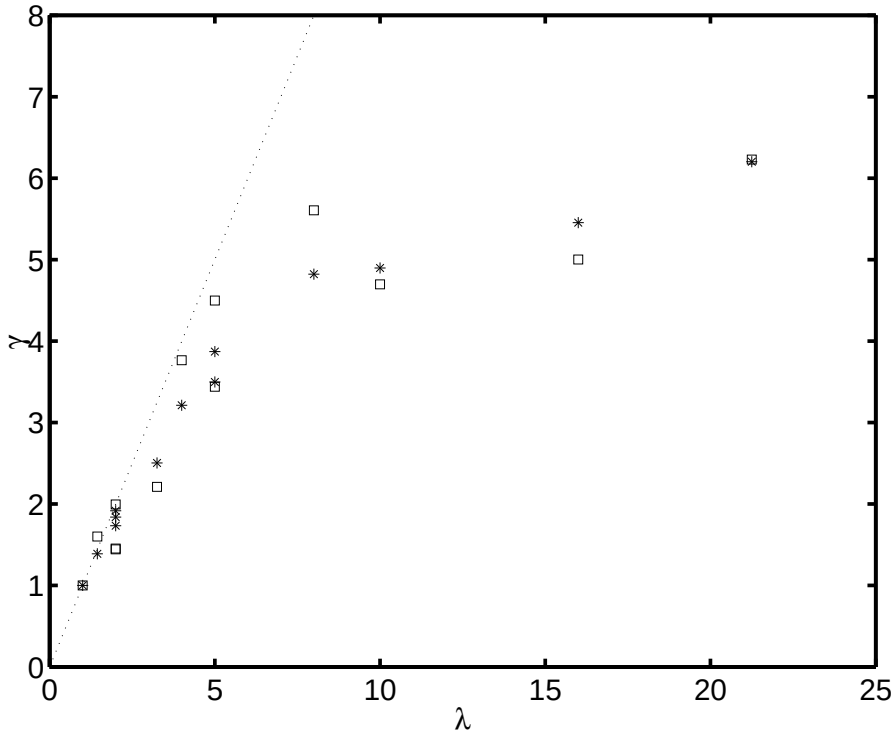

Figure 11: $\bar{\gamma}$ vs. λ ($\Box$). The dotted line is the prediction $\bar{\gamma} = \lambda$ and the stars are the prediction $\bar{\gamma} = \gamma\,(\kappa_m(t = 80))$

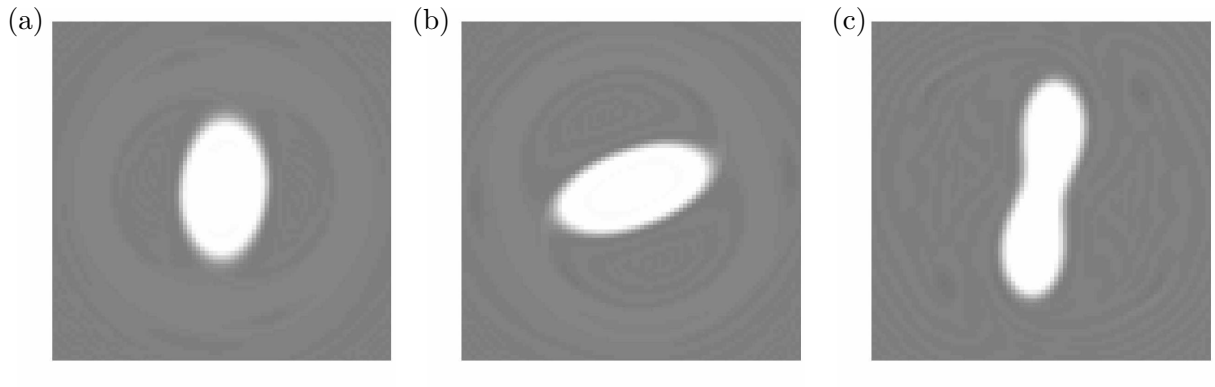

Figure 12: Vorticity field at $t = 20$ for an initially elliptical vortex with aspect ratio 8 for (a) one layer model, (b) $k_1 = 15$, $k_2 = 15$ and (c) $k_1 = 18, k_2 = 6$

be prototypical of the process of vortex merger [12]. Vortex merger is the major process controlling the evolution of a flow that is dominated by coherent vortices. We performed a series of simulations on the evolution of a single initially elliptical vortex in the model proposed here. While we have no quantitative results on the influence of finite-depth lower layers on vortex axisymmetrization, the qualitative differences are similar to those seen in the spin-down simulations. As λ increases, a given vortex undergoes less axisymmetrization, until for a critical value of λ there seems to be no trend at all to axisymmetrize, with wildly asymmetric vortex shapes persisting for long times (figure 12). Further characterization of the influence of k_R on the axisymmetrization process is also important.

5 Conclusion

The observation that initially motivated this investigation was of a correlation between the first Rossby deformation radius and the energy containing scales of the ocean circulation. Smith and Vallis showed that with surface-intensified stratification, such a correlation would be possible [4, 5]. Our model is much simpler, but can incorporate surface-intensified stratification by using deeper quiescent lower layers (i.e. $\lambda > 2$). We have shown that there is a scale-dependent slowing down of the evolution of this system. This slowing-down is a possible explanation for the build-up of energy at these scales in the ocean. In an equilibrium situation such as the ocean where input of energy at small scales is balanced by dissipation at large scales, retarded motion at a certain scale slows the inverse cascade of energy leading to an increased amount of energy at the retardation scale. To see quantitatively the effect of this in our model requires further simulations in the forced-dissipative equilibrium regime.

Further investigations of the evolution of the population of coherent vortices would give confirmation and additional understanding of the self-similar evolution and its slowdown at larger scales. To unify the spectral and physical space views of these equations, it would also be helpful to investigate the (physical space) interactions of individual vortices at a variety of length-scales. The study of the axisymmetrization of a single vortex and the

merger of two vortices would both be useful. Of particular interest is the effect of the finite lower layer depth on the critical merger separation for two vortices.

6 Acknowledgments

I would like to thank Oliver Bühler for the inspiration for and continual assistance with this work. Computational assistance was provided by Jeff Weiss, Keith Julien and Mark Petersen. The fellows of the 2003 GFD program also provided useful (and delicious) contributions.

References

[1] D. Stammer, "Global characteristics of ocean variability estimated from regional topex/poseidon altimeter measurements," J. Phys. Ocean. **27**, 1743 (1997).

[2] D. Stammer and C. Wunsch, in *Warm Water Sphere of the North Atlantic Ocean*, edited by W. Krauss (Gebrüder Bornträger, Berlin, 1996), pp. 159–194.

[3] A. Beckmann, C. W. Böning, B. Brügge, and D. Stammer, "On the generation and role of eddy variability in the central north atlantic ocean," J. Geophys. Res. **99**, 20381 (1994).

[4] K. S. Smith and G. K. Vallis, "The scales and equilibration of midocean eddies: Freely evolving flow," J. Phys. Ocean. **31**, 554 (2001).

[5] K. S. Smith and G. K. Vallis, "The scales and equilibration of midocean eddies: Forced-dissipative flow," J. Phys. Ocean. **32**, 1699 (2002).

[6] R. H. Kraichnan and D. Montgomery, "Two-dimensional turbulence," Reports on Progress in Physics **43**, 547 (1980).

[7] J. C. McWilliams, "The emergence of isolated coherent vortices in turbulent flow," J. Fluid Mech. **146**, 21 (1984).

[8] J. C. McWilliams, "The vortices of two-dimensional turbulence," J. Fluid Mech. **219**, 361 (1990).

[9] J. B. Weiss and J. C. McWilliams, "Temporal scaling behavior of decaying two-dimensional turbulence," Phys. Fluids A **5**, 608 (1993).

[10] A. Bracco, J. C. McWilliams, G. Murante, A. Provenzale, and J. B. Weiss, "Revisiting freely decaying two-dimensional turbulence at millenial resolution," Phys. Fluids **12**, 2931 (2000).

[11] A. Provenzale, "Transport by cooherent barotropic vortices," Ann. Rev. Fluid Mech. **31**, 55 (1999).

[12] M. V. Melander, N. J. Zabusky, and J. C. McWilliams, "Symmetric vortex merger in two dimensions: causes and conditions," J. Fluid Mech. **195**, 303 (1988).

[13] D. G. Dritschel and D. W. Waugh, "Quantification of the inelastic interaction of unequal vortices in two-dimensional vortex dynamics," Phys. Fluids A **4**, 1737 (1992).

[14] D. G. Dritschel, "A general theory for two-dimensional vortex interactions," J. Fluid Mech. **293**, 269 (1995).

[15] G. F. Carnevale, J. C. McWilliams, Y. Pomeau, J. B. Weiss, and W. R. Young, "Evolution of vortex statistics in two-dimensional turbulence," Phys. Rev. Lett. **66**, 2735 (1991).

[16] R. Salmon, *Lectures On Geophysical Fluid Dynamics* (Oxford University Press, New York, 1998).

[17] J. Pedlosky, *Geophysical Fluid Dynamics*, 2nd ed. (Springer Verlag, New York, 1987).

[18] L. M. Polvani, N. J. Zabusky, and G. R. Flierl, "Two-layer geostrophic vortex dynamics. part 1. upper v-states and merger," J. Fluid Mech. **205**, 215 (1989).

[19] V. D. Larichev and J. C. McWilliams, "Weakly decaying turbulence in an equivalent-barotropic fluid," Phys. Fluids A **3**, 938 (1991).

[20] N. Kukharkin, S. A. Orszag, and V. Yakhot, "Quasicrystallization of vortices in drift-wave turbulence," Phys. Rev. Lett. **75**, 2486 (1995).

[21] M. Arhan and A. Colin de Verdière, "Dynamics of eddy motion in the eastern north-atlantic," J. Phys. Ocean. **15**, 153 (1985).

[22] R. W. Griffiths and E. J. Hopfinger, "Coalescing of geostrophic vortices," J. Fluid Mech. **178**, 73 (1987).

[23] J. Verron, E. J. Hopfinger, and J. C. McWilliams, "Sensitivity to initial conditions in the merging of two layer baroclinic vortices," Phys. Fluids A **2**, 886 (1990).

[24] J. Verron and S. Valcke, "Scale-dependent merging of baroclinic vortices," J. Fluid Mech. **264**, 81 (1994).

[25] N. Hogg and H. Stommel, "The heton, an elementary interaction between discrete baroclinic geostrophic vortices and its implications concerning eddy heat-flow," Proc. Roy. Soc. London **397**, 1 (1985).